Microfluid Nanofluid (2015) 19:1019–1033
DOI 10.1007/s10404-015-1661-6

RESEARCH PAPER

Advances and challenges in computational research of micro- and nanoflows

Dimitris Drikakis[1] · **Michael Frank**[2]

Received: 26 February 2015 / Accepted: 27 September 2015 / Published online: 22 October 2015

Abstract This paper presents an overview of past and current research in computational modelling of micro- and nanofluidic systems with particular focus on recent advances in multiscale modelling. Different mesoscale and hybrid molecular–continuum methods are presented. The contributions of these methods to a broad range of applications, as well as the physical and computational modelling challenges associated with the development of these methods, are also discussed.

1 Introduction

Computational fluid dynamics modelling has long been performed using the Navier–Stokes equations, whose success in the design and optimisation of macroscopic structures and devices (e.g. aircraft, automobiles, buildings) has established it as an effective method for studying fluid flow. This continuum approach is based on the assumption of a continuum fluid, which is in equilibrium at any point or infinitesimal volume, a premise reasonable on larger scales.

However, the rapid technological advancements of the last half-century have enabled the manufacture and use of devices miniaturised within the micro- and nanoscale regime. Such applications range from microelectromechanical systems (MEMS) (Lyshevski 2005) and nanoelectronics (Yunus and Green 2010) to microchannel heat sinks (Tuckerman and Pease 1981). Additionally, many topics of academic and industrial interest have established a need to understand and exploit the behaviour of structures and matter from a nanometre point of view. Examples include nanocrystalline materials, biodetectors, drug delivery systems, and carbon allotropes, e.g. carbon nanotubes and graphene.

At small scales, fluids (and all states of matter) experience interfacial phenomena that affect a significant percentage of the overall system. In turn, the continuity required by traditional continuum approaches is compromised by steep gradients, rendering such techniques inadequate for the description of micro- and nanofluidic environments (Koplik et al. 1989; Travis et al. 1997; Wang et al. 2008).

The requirement for computations at finer resolutions is satisfied through atomic-scale simulation techniques such as molecular dynamics (MD) and the Monte Carlo (MC) method. Such models effectively delineate the physical apparatus, which governs the dynamics of such systems, assisting in the resolution of discrepancies between experimental results and macroscopic computational models. Examples include studies on the structure of the liquid particles close to the solid–liquid interface. These investigations found that the interactions between the solid walls and liquid form structured liquid layers close and parallel to the channel walls (see Fig. 1a) (Bitsanis et al. 1987; Asproulis and Drikakis 2010, 2011; Sofos et al. 2009). This reconciled experimental observations (Doerr et al. 1998; Henderson and van Swol 1984) and provided a better understanding of a phenomenon, which was correlated with properties of the system such as the stiffness of the wall and the strength of interaction between the wall and liquid atoms. The stratification of the liquid can ultimately

Michael Frank: On move to the University of Strathclyde.

✉ Dimitris Drikakis
dimitris.drikakis@strath.ac.uk

[1] Faculty of Engineering, University of Strathclyde, Royal College Bld, 204 George Str, Glasgow G1 1XW, Scotland, UK

[2] Fluid Mechanics and Computational Science, Cranfield University, Cranfield, Bedfordshire MK43 0AL, UK

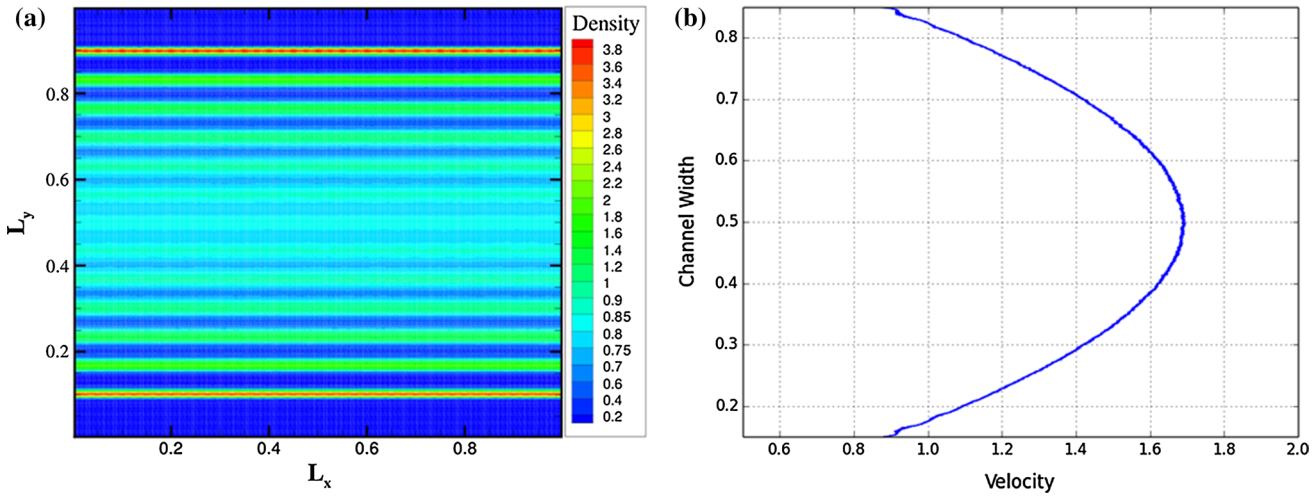

Fig. 1 Density (**a**) and velocity profiles (**b**) of a liquid in a nanochannel. **a** Density profiles of a fluid in a nanochannel. The walls of the channel are the thick, *dark blue slabs* on the *top* and *bottom* of the figure (where the density is zero since there are no liquid atoms). The liquid density is not uniform. Instead, it forms discrete, structured layers close and parallel to the channel walls. **b** Velocity profiles of flow in a nanochannel. It shows that at the solid–liquid interface, the velocity is not zero. This urges reconsideration of the no-slip condition commonly used in continuum approaches

change the properties of the system. An important example is the identification of a nonzero liquid velocity at the solid surface (Asproulis and Drikakis 2010, 2011) which, along with experimental data (Choi et al. 2003), has prompted a reconsideration of the circumstances under which the no-slip condition, often employed in macroscopic simulations, renders a physically meaningful constraint. The thermodynamics of nanofluidic scenarios have also been found to deviate from the expectations of continuum models. Flow through nanochannels has indicated the existence of a heat flux, even in the absence of a temperature gradient across the two walls, due to variations in the temperature profile arising from viscous heating (Baranyai et al. 1992; Todd and Evans 1997). Investigations have also studied the thermal resistance at the solid–liquid interface (Kapitza resistance), a phenomenon that is attributed to the different vibrational properties of the materials involved. These studies found that the thermal resistance is correlated with the wettability of the solid surface (Barrat and Chiaruttini 2003), the density of the liquid, and the wall stiffness (Kim et al. 2008). Investigations have also correlated the thermal conductivity of fluids with the size of the channel (Sofos et al. 2009). Researchers have also shown that under such spatial restrictions, the thermal conductivity is highly anisotropic between the parallel and the normal-to-the-wall directions. They associated this phenomenon to the reduced diffusion in the normal direction, due to the impaired motion and collision frequency of the liquid atoms associated with confinement (Liu et al. 2005).

The main issue in atomic-scale simulations is the computational cost, which increases significantly with the size of the simulation domain. Hence, complications arise in microflows in which the non-homogeneities and interfacial effects of nanoflows are still evident, rendering continuum mechanics inadequate, yet the system size is outside the practical scope of MD.

This blend of difficulties in such systems renders the independent use of either continuum or atomistic methods insufficient or practically impossible. To account for this, mesoscale and hybrid molecular–continuum methods (HMCM) have been of academic interest for over two decades now. These approaches attempt to bridge the two types of models into a synergy, which allows for an accurate calculation of the properties of the system at a relatively low computational cost. Mesoscale models comprise a single solver, which attempts to give a more efficient solution based on atomistic observations, while HMCM utilise both molecular and continuum solvers that exchange information. Figure 2 shows the time and length scales in which quantum, atomistic, continuum, and hybrid methods are used.

The paper is organised as follows: Sect. 2 briefly describes the MD method and immediately continues with a paragraph on the continuum model since both methods are the building blocks for the multiscale methods for which the discussion follows later on. Since the continuum model is based on the average behaviour of atoms and molecules, it was deemed more intuitive to present the MD approach first followed by the continuum one. The aim of this section is to provide the reader with the strengths and limitations of these approaches, highlighting the need for multiscale modelling. Section 3 discusses some popular

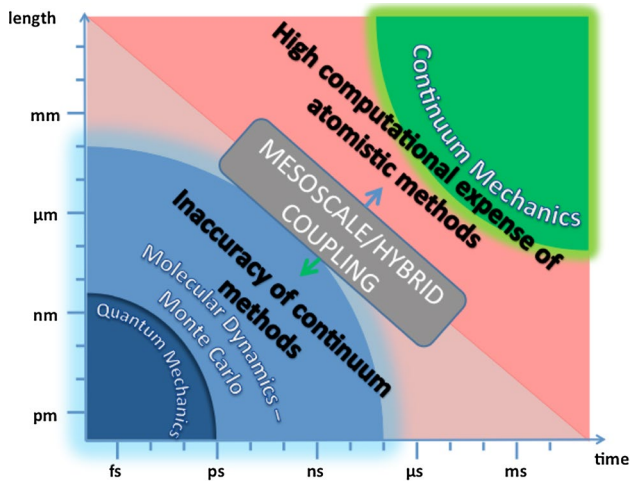

Fig. 2 Time and length scales of computational methods for micro- and nanofluids

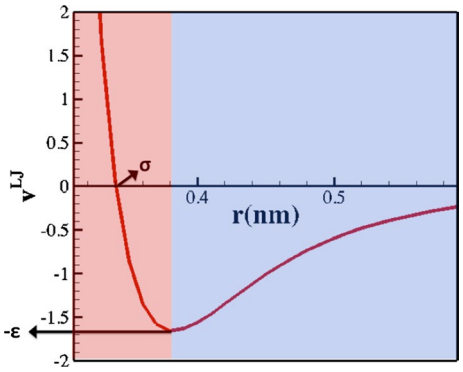

Fig. 3 The Lennard-Jones potential. The *red-shaded* area corresponds to the strong repulsive forces, a product of the Pauli exclusion principle, whereas the *blue-shaded* area corresponds to the attractive London dispersion forces

mesoscale approaches, independent methods of intermediate resolution attempting to overcome the problems of the purely molecular or continuum methods. The strengths and limitations of each method are also discussed. Section 4 discusses hybrid multiscale methods. As the name suggests, these utilise both a continuum and a molecular solver to address different physical scales. We categorise these methods depending on how the system is decomposed into molecular and continuum components and how information is exchanged between the atomistic and continuum solvers.

Section 5 summarises the conclusions drawn from the present work.

2 Computational methods

2.1 Molecular dynamics

Molecular dynamics (MD) is a deterministic computational method, which calculates the trajectory of all atoms in time. Given the atomic positions $\boldsymbol{r}$ and velocities $\mathbf{v}$, the system is evolved through Newton's equations of motion

$$\dot{\boldsymbol{r}}_i = \boldsymbol{v}_i, \quad F_i = m_i \dot{v}_i, \tag{2.1}$$

where the index i represents and arbitrary particle (atom or molecule) and $\boldsymbol{F}_i$ is the force acting on the particle, determined by

$$\boldsymbol{F}_i = -\nabla \mathcal{V} = -\frac{\partial}{\partial r}\mathcal{V}, \tag{2.2}$$

where $\mathcal{V}$ is the total potential energy of the system, which depends on the relative positioning of all the atoms, as well as the nature of the intermolecular and intramolecular interactions in the system. An accurate description of this potential is within the scope of quantum electrodynamics. However, MD uses empirical functions that can accurately portray the atomic interactions. A popular pairwise potential that MD simulations often use for non-bonded van der Waals interactions is the Lennard-Jones (LJ) potential given by the function

$$V^{LJ} = 4\varepsilon\left[\left(\frac{\sigma}{\boldsymbol{r}}\right)^{12} + \left(\frac{\sigma}{\boldsymbol{r}}\right)^{6}\right]$$

where ε is the depth of the potential well and σ is the point of intersection with the interatomic distance axis (Fig. 3). As Fig. 3 shows, at small interatomic distances, a strong repulsive force is acting on the two atoms, which tends to infinity as their separation approaches zero. This corresponds to the Pauli exclusion principle, which prevents the electron shells of the particles from overlapping. The blue-shaded region in the figure corresponds to the attractive London dispersion forces acting between non-reacting gases such as argon.

The reason for the crippling computational expense of MD is twofold. Firstly, as the systems scale to practically meaningful dimensions, the number of atoms increases significantly. Even if a pairwise potential is used, the runtime increases beyond the capabilities of modern computing. Secondly, the time step used in the simulations should be small in order to ensure that the atomic positions vary smoothly with time. This is especially true when we consider systems with high temperatures or rapidly varying potentials, such as that depicted in Fig. 3, where a large time step can result in unnatural atomic overlapping and, in turn, cause velocity discontinuities and degrade the energy-conserving properties of the system (Allen and Tildesley 1989).

Therefore, the objective of all mesoscale and multiscale approaches is to decouple the microscopic spatial and timescales from a large part of the domain, thus allowing

the simulations to be performed within more realistic timescales.

2.2 Continuum model

The continuum model does not treat systems as a collection of atomic trajectories. Instead, the primitive state variables such as density ρ, flow velocity $\boldsymbol{u}$, energy e, temperature T, and pressure p are considered as functions of time and space, averaged over a large number of atoms (e.g. $\rho = \rho(x, y, z, t)$ in Cartesian co-ordinates).

The behaviour of fluids in this continuum approach is governed by the Navier–Stokes equations, a set of three equations based on the conservation of mass, momentum, and energy, given by

$$\frac{\partial \rho}{\partial t} = -\nabla \cdot (\rho u) \tag{2.3}$$

$$\frac{\partial \rho \boldsymbol{u}}{\partial t} = -\nabla \cdot (\rho \boldsymbol{u} \otimes \boldsymbol{u}) - \nabla \cdot \Pi \tag{2.4}$$

$$\frac{\partial e}{\partial t} = -\nabla \cdot (e\boldsymbol{u}) - \nabla \cdot (\Pi \cdot \boldsymbol{u}) - \nabla \cdot \mathbf{q} \tag{2.5}$$

where the stress tensor $\mathbf{\Pi}$ of a Newtonian fluid is empirically given by

$$\mathbf{\Pi} = \mathrm{p}\mathbf{I} - \boldsymbol{\lambda}_v(\nabla \cdot u)\boldsymbol{I} - \mu\left[(\nabla \boldsymbol{u}) + (\nabla \boldsymbol{u})^{\boldsymbol{T}}\right] \tag{2.6}$$

the heat flux vector $\boldsymbol{q}$ is given by

$$\boldsymbol{q} = \boldsymbol{\lambda}\nabla \mathrm{T} \tag{2.7}$$

and the equations of state for p and T are given by

$$p = p(\rho, e_i) \text{ and } T = T(\rho, e_i) \tag{2.8}$$

3 Mesoscale methods

In an attempt to bridge the microscopic and macroscopic environments, mesoscale methods provide a framework of intermediate resolution. They are based on the often correct assumption that the behaviour of every single atom is not required to produce realistic results. Instead, large numbers of molecules are grouped together. Within the scope of mesoscale methods, these pseudo-particles are considered fundamental and interact among themselves without considering the influence of their constituent atoms.

3.1 Lattice gas automaton

One of the first mesoscale approaches to simulating gases is the lattice gas automaton (LGA) method (Pomeau and Frisch 1986; Wolfram 1986; Hardy et al. 1973). As the

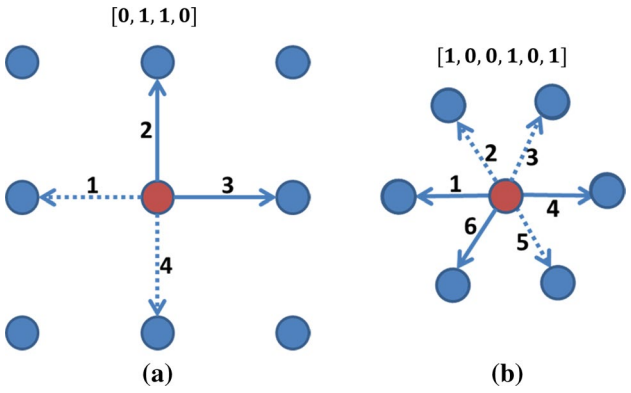

Fig. 4 Boolean representation of a lattice point (*red node*) **a** for a square lattice and **b** for a hexagonal lattice. The *arrows* indicate the possible velocities. A *solid line* suggests that the *red lattice* site has an atom moving in that direction, while a *dashed line* indicates that there is no particle with that velocity on that point. **a** Square lattice, **b** hexagonal lattice

name suggests, a lattice covers the system and gas particles can only be positioned on the lattice sites. Each particle can only move along the lattice links (i.e. lattice vectors), which are a characteristic of the lattice used. The model defines the velocity of each atom based on the lattice link along which it will move on to the next time step to reach a neighbouring point. Each lattice site can hold a number of atoms equal to the number of lattice links attached to it. Furthermore, two atoms on the same point cannot have the same velocity (i.e. two atoms on the same point cannot travel in the same direction). This facilitates the representation of each lattice point by a Boolean vector with a dimension equal to the number of possible directions (i.e. lattice links) from each node. For each direction, the value is 1 if there is an atom on that point moving with that velocity.

In order to illustrate the above, Fig. 4a shows one possible configuration of atoms (chosen arbitrarily) found on a lattice site (the red circle) on a square lattice. The arrows indicate the possible values of the velocity. A solid line means that an atom moving in that direction is located on the lattice point, while a dotted line suggests that such an atom is absent. Since the velocity can take four values, a four-dimensional vector is used to describe the state of the node. Since there is no atom moving in direction 1 and 4 (suggested by the dotted lines in those directions), the corresponding components in the vector are 0. On the other hand, the third and fourth components have a value of one, indicating that there are two atoms moving in directions 3 and 4.

At each time step, LGA carries out two operations:

1. *Propagation*. During this step, the particles are moved to nearby lattices depending on their velocities of the previous time step. For example, in Fig. 4a the atom

with velocity 2 will move to the top vertex, pointed by the arrow, in the next time step. As we have mentioned earlier in this section, two atoms located at the same point cannot move along the same direction.

2. *Collision*. If two particles arrive at the same lattice point, a collision is detected and the velocities must be readjusted. Depending on the implementation of the algorithm, a set of collision rules are used to adjust the velocities of the colliding atoms. The redistribution of velocities must conserve mass and momentum. The new velocities will reflect the direction of motion of the particles in the next step. However, when two atoms are using the same link with opposite velocities, a collision is not detected and the atoms move freely to swap lattice sites.

This seemingly simplistic model can potentially reproduce the Navier–Stokes equations by taking averages over a large number of nodes. This, however, requires a lattice with sufficient symmetry. The fourfold symmetry of the lattice depicted in Fig. 4a is incapable of reproducing the hydrodynamic equations. For two-dimensional systems, the symmetry of the hexagonal lattice illustrated in Fig. 4b is indeed sufficient. Such a system allows the atoms to move in six directions. To accommodate this, we require six-dimensional vectors to store the state of each lattice point at each time step. In addition, more collision rules are required as particles can now collide at more angles. Hydrodynamic lattices are also available for three-dimensional systems.

Finally, it is worth mentioning the key differences between MD and LGA since both methods consider interacting particles. MD is gridless and therefore does not restrict the motion of atoms. Additionally, as we have mentioned in Sect. 2.1, MD considers microscopic interactions, which classically approximate quantum mechanical behaviour as accurately as possible. This gives rise to realistic equations of state, whereas the collision rules of LGA only facilitate isothermal relationships between mass, density, and pressure. However, the simplicity of LGA models is accompanied by a very attractive computational efficiency, which is of course the objective of multiscale models.

3.2 Lattice Boltzmann method

The appealing computational simplicity of the Boolean nature of LGA methods is inevitably accompanied by numerical noise. For example, since an atom with a specific discrete velocity can either exist (1) or not (0) on each node, its density, calculated as the number of atoms on each node (i.e. the sum of 1s on the Boolean vector), can only have an integer value. Averaging over a large number of nodes can reduce this noise but costs computationally. The Lattice Boltzmann (LB) method (McNamara and Zanetti 1988; Chen and Doolen 1998) attempts to resolve these issues by storing the real particle density at each lattice point. Furthermore, although the particles can travel along the lattice directions, as in LGA, a real number of particles on each lattice site occupy each of them. Therefore, the density and velocity of the fluid at a certain position along a certain direction are given by

$$\rho(\boldsymbol{x}) = \sum_i f_i(\boldsymbol{x}) \tag{3.1}$$

$$u(\boldsymbol{x}) = \sum_i f_i(\boldsymbol{x})\boldsymbol{c}_i \tag{3.2}$$

where $\boldsymbol{x}$ is the lattice point, i is an arbitrary lattice direction, $f_i(\boldsymbol{x}, t)$ is the portion of the density of the lattice site moving in a lattice direction, and $\boldsymbol{c}_i$ is the corresponding lattice vector.

As in the LGA models, the evolution of the system consists of a propagation and collision step. The propagation step is given by

$$f_i(\boldsymbol{x} + \boldsymbol{c}_i\Delta t, t + \Delta t) = f_i(\boldsymbol{x}, t)$$

simply stating that the density distribution in a certain direction at a node inherits that of its neighbour (along the vector $\boldsymbol{c}_i$) from the previous time step. Accounting for collisions, the full equation becomes

$$f_i(\boldsymbol{x} + \boldsymbol{c}_i\Delta t, t + \Delta t) - f_i(\boldsymbol{x}, t) = \Omega_i(f) \tag{3.3}$$

where Ω is the collision operator and $\boldsymbol{c}_i$ are the lattice-restricted velocities.

Due to the additional complexity of LB models in comparison with LGA, more complicated collision operators are required. This is usually approximated by the Bhatnagar–Gross–Krook (BGK) operator given by (Bhatnagar et al. 1954)

$$\Omega : f_i \rightarrow -\frac{1}{\tau}\left[f_i - f_i^{\mathrm{eq}}\right] \tag{3.4}$$

where f_i^{eq} is the equilibrium particle distribution based on the discretised version of the Maxwell–Boltzmann equilibrium distribution (Qian et al. 1992).

LBM can also treat physical phenomena where body forces are involved. Such cases include multiphase and multicomponent systems. This, however, requires the addition of the force to the evolution equation (Eq. 3.3) and that the velocity and equilibrium distribution are adjusted accordingly (Guo et al. 2002a, b).

The base model described above can be modified to accommodate various flow phenomena. For Poiseuille flow, the collision rules at the solid–liquid interface are adapted so that fluid particles arriving at the boundary are bounced back by inverting the lattice velocity (Succi 2001).

For Couette flow, this model is adjusted so that part of the boundary momentum is injected into the bounced fluid (Ladd 1994). This approach models the boundaries at lattice link midpoints and is therefore unable to capture the behaviour of arbitrarily curved surfaces. Subsequent studies have proposed extensions to these models to account for more complex geometries (Filippova and Hänel 1998; Guo et al. 2002a, b).

LBM has also been adapted to accommodate inlet and outlet boundaries. There are two main types of problems with different models for each. The first type is when the velocity and density are known at the inlet and outlet, respectively (Zou and He 1997; Izquierdo et al. 2009). The second is when both the velocity and density are known at the inlet, and the flow at the outlet is considered fully developed (Yu et al. 2005).

The method also enables simulations of complex and multiphase flows by modelling potential interactions between the pseudo-particles. This is achieved by defining an external force, which acts on f_i^{eq}. The mesoscale interactions can naturally give rise to non-ideal fluid. This allows for simulation of complex systems such as the effect of gas bubbles on the liquid slippage at a rough solid surface (Hyvaluoma and Harting 2008). To realise such effects, the free-energy functional of the system is considered, giving rise to a pressure tensor that can be included in f_i^{eq} (Swift et al. 1995).

An alternative method is to include an interaction term between the pseudo-particles, given by (Shan and Chen 1994)

$$F(x) = \psi(\boldsymbol{x}) \sum_i g_i G \psi(\boldsymbol{x} + \psi(\boldsymbol{x} + \boldsymbol{c_i})\boldsymbol{c_i}) \tag{3.5}$$

where G is the ratio of the potential to thermal energy, $\psi(\boldsymbol{x})$ is the potential that describes the interactions of the pseudo-particles under inhomogeneities, and g_i is a lattice-dependent weighting factor dividing the force among the various lattice directions. Adjusting the equilibrium distributions based on the effects of this force on the velocity provides an equation of state, which for high values of G resembles the van der Waals equation, enabling the simulation of liquid–gas interfaces. Although the thermodynamic validity of this pseudo-potential scheme has been criticised as it is not derived from a free-energy functional, it has been proved effective in successfully describing various systems. Furthermore, the addition of a gradient force in Eq. 3.5 can bridge these thermodynamic inconsistencies (Sbragaglia et al. 2009).

3.3 Dissipative particle dynamics

Dissipative particle dynamics (DPD) is a mesoscale approach in which, unlike LGA and LB, pseudo-particles move continuously in space rather than jumping across points on a lattice (Hoogerbrugge and Koelman 1992). These bodies represent groups of atoms or subthermodynamic ensembles and interact among themselves through pairwise interactions. In this sense, DPD can be considered as a coarse-grain equivalent of MD. Each pseudo-particle moves in free space. Its momentum is updated every time step according to the force acting on it given by

$$F_i = \sum_{i \neq j} \left(F_{ij}^{\mathrm{C}} + F_{ij}^{\mathrm{D}} + F_{ij}^{\mathrm{R}} \right) \tag{3.6}$$

The term F_{ij}^{C} is a purely repulsive, conservative force that prevents major overlaps between the particles. This component acts in the same way as the repulsive component of the non-bonded potentials that MD employs (e.g. Lennard-Jones potentials). However, the more complicated potentials of microscopic simulations produce forces that increase to infinity as the interatomic distance approaches zero. As we have mentioned in Sect. 2.1, this severely restricts the maximum time step that can be used. However, if we average these interactions over large groups of atoms, such as in DPD, a "softer" potential can be used which is finite even at zero separation. This allows the use of a much larger time step, a very attractive quality of this mesoscale method that allows the simulation of more practical systems. The dissipative (F_{ij}^{D}) force describes viscous, frictional forces, and it is a function of interatomic distances and relative velocities between atoms in the system. Finally, the term F_{ij}^{R} is a stochastic force that introduces Brownian motion. The dissipative and random forces emulate the internal degrees of freedom (i.e. the atomic fluctuations within the pseudo-particles) of these mesoscale particles and regulate the temperature (they act as a Langevin thermostat). Once the force is defined, Newton's second law of motion (Eq. 2.1) is used for advancing the trajectory of the system through phase space. The conservative force is then given by

$$F_{ij}^{\mathrm{C}} = a_{ij} w^{\mathrm{C}}(r) \boldsymbol{r}_{ij} \tag{3.7}$$

where a_{ij} is the maximum repulsion between the dissipative particle i and j, r is their interatomic distance, and $w^{\mathrm{C}}(r)$ is a weight function, often set to

$$w^{\mathrm{C}}(\boldsymbol{r}) \begin{cases} (1 - r) & r < 1.0 \\ 0 & r \geq 1.0 \end{cases} \tag{3.8}$$

This formulation only includes a repulsive component. Although this is an accurate approximation of gases, for more complex systems such as multiphase flow, an attractive component should also be added. In this case, the weight function can be given by (Liu et al. 2006, 2007)

$$w^{\mathrm{C}}(\boldsymbol{r}) = -\left[A W_1'(r, r_{c1}) - B W_2'(r, r_{c2}) \right] \tag{3.9}$$

where $W_1(r, r_{c1})$ and $W_2(r, r_{c2})$ are spline functions representing the repulsive and attractive interactions; A and B define their strengths; and r_{c1} and r_{c2} are their cut-off distances.

Modelling stationary solid surfaces can be achieved by fixing or freezing the pseudo-solid particles (as is the case with MD). The solid–liquid interactions must be modelled accordingly to prevent liquid atoms from penetrating the solid walls. Although this can be achieved by increasing the solid density as well as assigning a greater repulsive interaction between the two phases, such methods have presented inaccurate physical behaviour (Kong et al. 1994; Jones et al. 1999; Willemsen et al. 2000). Instead, reflection algorithms can be used to reverse the velocity of the fluid particles, in a manner similar to LBM (Revenga et al. 1998).

4 Hybrid molecular–continuum methods

An alternative method for dealing with systems at micro-scales is the HMCM in which both molecular (usually MD or MC) and continuum (usually CFD and FEM) solvers are used (Kalweit and Drikakis 2011). The basic principle behind these hybrid techniques is to limit the use of the molecular solver as much as possible. The size of the domain (i.e. number of atoms) is the biggest bottleneck in molecular methods. Therefore, all HMCM decouple the length scales by running molecular simulations in one or more subdomains, small relative to the overall size of the system. In addition, some HMCM decouple the timescales by running the molecular simulations for only selected periods. Figure 5 illustrates a general categorisation of the available HMCM. Geometric decomposition and pointwise coupling are based on how the model allocates the system to the molecular and continuum solvers. Geometric decomposition divides the system spatially and exclusively allocates one of the two solvers for each region. The appropriate exchange of information between them, either state variables or fluxes, ensures transparency of the computational division and continuity in the physics of the system. On the other hand, the pointwise coupling method solves the entire system in a continuous fashion and uses microscopic refinement around the grid points. Although all HMCM decouple the length scales, only some of them decouple the macroscopic and microscopic timescales. Note that employing equilibrium kinetic theory concepts to what is definitely a non-equilibrium process should be borne in mind when considering the limitations of multi-scale methods. Although this is recognised by the present authors, it is an issue that requires further elaboration that is beyond the scope of the present study. The aforementioned methods are discussed in more detail below.

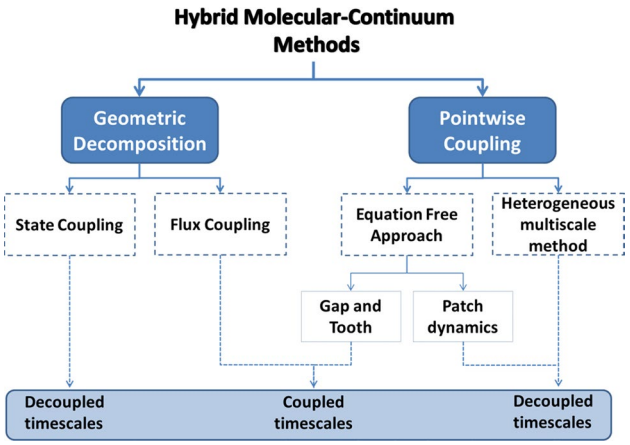

Fig. 5 General classification of hybrid molecular–continuum methods (HMCM). Geometric decomposition and pointwise coupling differ with respect to the implementation of the molecular and continuum solvers in the simulation box

4.1 Geometric decomposition

Geometric decomposition (GD) refers to a HMCM in which the simulation domain is decomposed into regions, some of which are dealt with by the molecular and others by the continuum solver. As the objective of such hybrid methods is to minimise computational resources, the higher-resolution molecular regions should be much smaller than the continuum regions.

The continuity of thermodynamic and transport properties between the various parts of the system is integral in modelling a physically accurate environment. It is therefore crucial to define a protocol in which the two solvers share information with each other and adjust in order to conform to the laws of physics. This is achieved by defining an overlapping region near the interface of the two regions, called hybrid solution interface (HSI), which is treated by both the continuous and molecular components.

Figure 6 shows the process behind GD. The continuum region on the left, highlighted in light blue, is solved using a finite volume method and is therefore divided into cells. The grid is extended slightly into the molecular domain. The coinciding cells are called ghost cells. Although the domain in molecular methods is not traditionally divided into a grid, virtual cells are defined which coincide with the ghost cells of the continuum solver. This sets up a framework enabling the exchange of information between the two.

The coupling of the solvers is bidirectional. The molecular component calculates properties within the virtual cells and imposes them onto the ghost cells. In turn, these will adjust the boundary cells (dark blue cells in Fig. 6). On the other hand, macroscopic properties in the ghost cells are

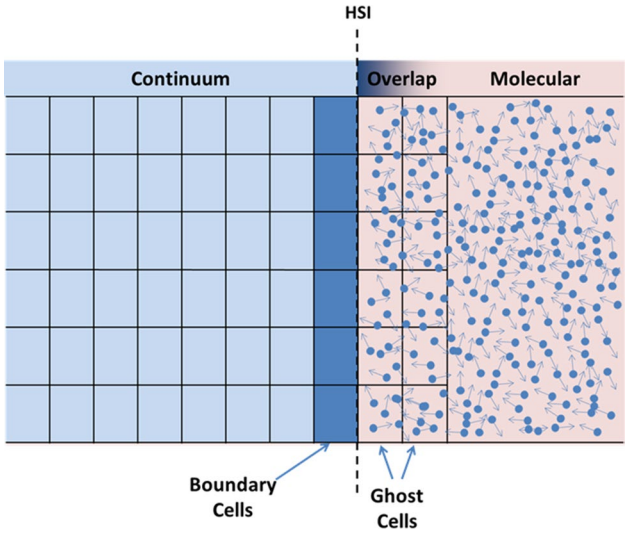

Fig. 6 Schematic representation of GD

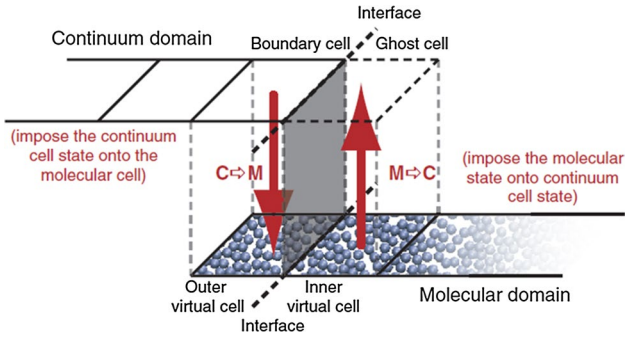

Fig. 7 A one-dimensional illustration of coupling by states in both directions. The continuum and molecular domains are separated to aid visualisation. The *arrows* symbolise the transfer of states from the continuum to the molecular domain (C → M) and vice versa (M → C)

imposed onto the molecular domain by adjusting the number and velocities of the atoms within the corresponding virtual cells.

The protocol at the HSI varies significantly between GD implementations. However, all GD schemes need to satisfy a set of fundamental requirements, namely:

- The conservation laws of mass, momentum, and energy should hold across the boundary.
- The state variables across the boundary must portray a physically accurate behaviour. This means that by looking at the flow solution of the simulation (i.e. density profiles), the position of the HSI should not be identifiable.

The coupling must be also designed in the most simplistic and computationally efficient manner possible.

GD can differ in the type of information used for coupling the two solvers. Two broad categories can be identified

1. State coupling
2. Flux coupling

These will be discussed in the sections below.

4.1.1 State coupling

State coupling refers to the sharing of state variables such as density, temperature, and velocity, across the HSI. Figure 7 illustrates a one-dimensional set-up for coupling by states with the continuum region being on the left and the molecular region on the right. The vertical separation is merely an artefact to aid in the visual clarity of the figure.

As already mentioned, this exchange of information occurs from the continuum to the molecular region and vice versa. The transfer of data from the molecular to the continuum domain is not so complicated since the macroscopic quantities can be obtained through spatial and temporal averaging of the atomic behaviour. In general, a state variable $\mathcal{A}$ has an instantaneous value, obtained by averaging the behaviour of many atoms at an arbitrary instance. As a statistical quantity, this value can fluctuate significantly across different points in time. The reduction in these fluctuations is achieved through averaging the instantaneous calculations over a suitably long timescale by:

$$\langle \mathcal{A} \rangle_t = \frac{1}{\delta t} \int_{t_0}^{t_0+\delta t} \mathcal{A}(t) \mathrm{d}t, \tag{4.1}$$

where $\langle \mathcal{A} \rangle_t$ denotes the time average of the quantity $\mathcal{A}$; t_0 denotes the initial time frame in which the value is calculated; δt is the timescale over which the quantity is averaged; and $\mathcal{A}(t)$ is the instantaneous calculation. For computational purposes, the equation can be written in discrete form as

$$\langle \mathcal{A} \rangle_t = \frac{1}{N_\mathrm{t}} \sum_{\tau=0}^{N_t} \mathcal{A}(t), \tag{4.2}$$

where τ denotes the time step of the molecular simulation and N_t is the number of time steps used for the averaging. The ghost and boundary cells can trivially inherit the calculated values.

Transferring information from the continuum to the molecular domain is a more complicated task. The difficulty arises from the requirement to construct a microscopic state of 6 N degrees of freedom (momentum and

position of N atoms) from the macroscopic state, with only five degrees of freedom (ρ, $\boldsymbol{u}$, and e) (Asproulis et al. 2009). This interpolation requires additional assumptions or stochastically generated values.

For incompressible flows, this is achieved by matching the atomic number density and average velocity in the HSI with the corresponding continuum values. Inserting or deleting atoms in the virtual cells controls the density. The momentum is coupled by rescaling the atomic velocities accordingly. The temperature can also be regulated based on the equipartition theorem, according to the equation

$$T = \frac{2}{3\kappa_{\mathrm{B}}}\bar{e}_{\mathrm{k}} \tag{4.3}$$

where $\bar{e}_{\mathrm{k}}$ is the average kinetic energy of all atoms about their mean position, i.e. excluding the kinetic energy of the centre of mass within that cell, and κ_{B} is the Boltzmann constant.

State coupling becomes much more complicated for compressible flows as the positions and momenta of the atoms must also match the continuum energy. Although in its own right this is not a difficult task, the abundance of microscopic states fulfilling this constraint must further be reduced to those maximising the entropy of the system and, in turn, satisfy the second law of thermodynamics. Such a task greatly increases the computational complexity of the algorithm, a highly undesirable outcome.

Initially, MD–CFD-based state coupling methods were used to study 1D incompressible Couette flow, which did not permit mass or energy transfer across the HSI (O'Connell and Thompson 1995). The molecular and continuum environments were coupled by exchanging velocities using constrained Lagrangian dynamics. A 2D state coupling scheme was proposed shortly after for the study of Poiseuille and Couette flows of supercritical argon (Hadjiconstantinou and Patera 1997) and the moving contact line problem (Hadjiconstantinou 1999). The method allowed mass flow across the MD/CFD interface by enclosing the molecular region within a bigger simulation box with periodic boundary conditions serving as a particle reservoir. More recent advances in state coupling, MD–CFD methods emulated mass flow by inserting and deleting particles that cross the HSI (Werder et al. 2005). The model has been used to study flow of a LJ fluid around a carbon nanotube (CNT), the results of which agreed with those similar cases treated exclusively with MD. State coupling methods suitable for unsteady flows have also been derived (Liu et al. 2008).

Methods for reducing the noise resulting from the thermal fluctuations in the molecular domain have also been proposed (Ko et al. 2014). This has been achieved by sampling the state variables from multiple, replicated molecular systems set at different initial conditions. Furthermore, by spatial and temporal regressions, a more accurate exchange of variables can be achieved.

4.1.2 Flux coupling

Rather than exchanging information on the state of each region, flux coupling methods update the state variables by monitoring the inflow and outflow of mass, momentum, and energy. The monitoring is required to account for all ways in which quantities can be transported. Mass can only be transferred through *convection*, the bulk motion of fluid particles. Momentum can be transferred by both convection and the *stresses* applied on atoms by their neighbours. Finally, energy can be transferred by convection, through interatomic stresses, as well as through *conduction*.

As in the case of state coupling, the transfer of information from the molecular to the continuum domain is simpler than the inverse exchange (continuum to molecular). We achieve this by monitoring and calculating the flow of a quantity through a virtual cell face within the overlapping region or an arbitrary volume enclosing the surface. This flow can then be imposed on the corresponding ghost cells (or corresponding volume enclosing the ghost cell's face). This can be seen in Fig. 8 where the vertical, black, dashed line indicates the face of the cell. Figure 8a illustrates that the flux is measured by the rate in which atoms or molecules cross this surface. In Fig. 8b, the shaded red region is the volume containing the surface, in which the fluxes are calculated. Once the atomic trajectories are translated into fluxes (again through the use of statistical mechanics), and time-averaged, as shown in Eq. 4.2, the fluxes are imposed onto the continuum region.

The exchange of fluxes from the continuum to the molecular domain is again more complicated as the fluxes in and out of the ghost cells must be mapped onto the virtual cells. To account for convective fluxes, atoms are inserted or deleted in the virtual cells of the HIS. The number of atoms regulates the mass transfer, and their velocities control the convective momentum and energy transfer. In

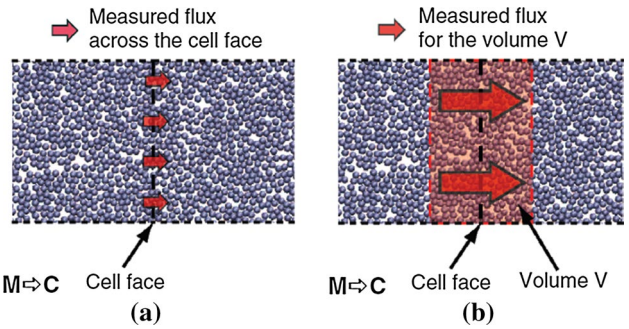

Fig. 8 Schematic representation of flux coupling. **a** Across cell, **b** across volume

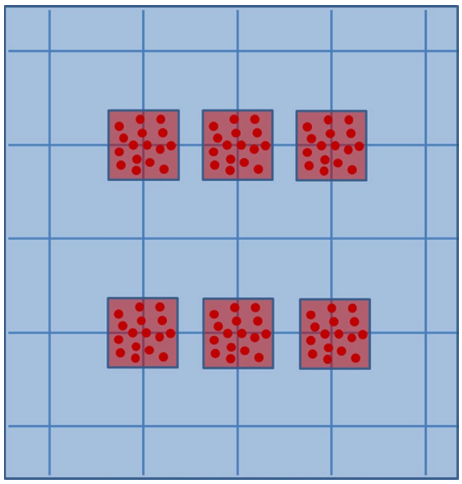

Fig. 9 A schematic illustration of length decoupling in PWC

order to impose momentum transfer through stress, appropriate force fields are applied onto the atoms. Finally, the conductive flux can be realised by rescaling the velocities of the atoms, emulating energy transfer.

Incompressible, isothermal flows are significantly simpler than compressible cases as the two energy fluxes (stress and conductive) can be ignored (Hadjiconstantinou and Patera 1997; Barsky et al. 2004; De Fabritiis et al. 2007). However, all fluxes can be incorporated into the molecular domain, allowing for the simulation of compressible flows (Delgado-Buscalioni and Coveney 2003a). Additionally, this method is suitable for phenomena whose characteristic timescales are comparable to molecular timescales, such as waves (Delgado-Buscalioni et al. 2005; De Fabritiis et al. 2007). However, due to the constant need to monitor the fluxes across the molecular and continuum regions, GD flux coupling methods do not decouple timescales and are, therefore, not preferred by some authors (Wijesinghe and Hadjiconstantinou 2004; Koumoutsakos 2005).

Researchers initially used flux coupling methods to study incompressible flows (Flekkøy et al. 2000; Wagner et al. 2002). Mass and momentum fluxes were exchanged within the HSI by having a reservoir around the MD region, in which atoms were either inserted or deleted, emulating in- and outflow. The model was further extended to account for compressible flows by incorporating the coupling of energy fluxes (Delgado-Buscalioni and Coveney 2003a). This was later improved by introducing an algorithm for inserting atoms (Delgado-Buscalioni and Coveney 2003b) and even polar molecules, such as water (De Fabritiis et al. 2004) to achieve the desired energy levels. The applicability of this flux coupling approach has rendered it the preferred method for various researchers (Delgado-Buscalioni and Coveney 2003b; Flekkøy et al. 2000). The method was applied on incompressible isothermal flows over an oscillatory wall (Delgado-Buscalioni and Coveney 2004) and, successfully, simulated single tethered polymer in a solvent, subjected to oscillatory flow (Barsky et al. 2004). Past studies have investigated the boundary conditions used in the flux

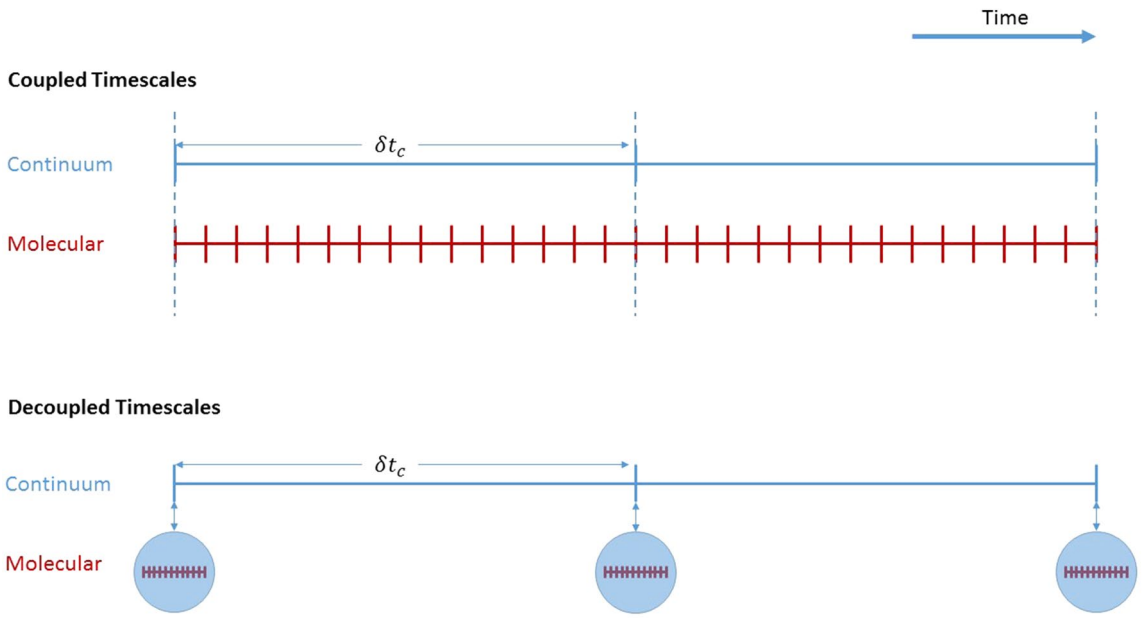

Fig. 10 A schematic illustration of time decoupling in PWC. For coupled timescales, the molecular and continuum simulations run in parallel. For decoupled timescales, the molecular simulation runs for a number of microscopic time steps at specific macro-time steps

coupling approaches attempting to smoothen any numerical artefacts and discontinuities induced at the HSI (Kalweit and Drikakis 2008a, b, 2010). Extensions to the flux coupling models have been proposed to take into account the fluctuations of state variables when transferring information from the molecular to the continuum region. This can be achieved by adapting the macroscopic equations as well as by implementing a relatively fine grid near the HSI. Such flux coupling methods have successfully simulated sound waves propagating through water and reflected by a lipid monolayer (Delgado-Buscalioni et al. 2005; De Fabritiis et al. 2007). Previous investigations have also used GD to couple fluxes from the continuum to the molecular domain in connection with the study of dynamic friction between crystal silver on copper at high pressure (Barton et al. 2011).

4.2 Pointwise coupling

Rather than having regions treated exclusively by a molecular or continuum solver (as is the case with GD), the pointwise coupling (PWC) solves the entire domain using the continuum solver, with the molecular component acting as a refinement by providing information used for more accurate calculations (Asproulis et al. 2012). There are two types of problems in which such methods are effective:

(a) Problems in which the boundary conditions (e.g. velocity slip) need to be resolved by the microscopic solver;
(b) Problems in which the constituent relations need to be extracted from the molecular models.

Running molecular simulations in regions small compared to the continuum cell size decouples the length scales (Fig. 9). In addition, PWC decouples timescales by computing the microscopic information in small bursts, i.e. a small number of time steps (Fig. 10).

The entire domain is solved by the continuum model (blue), while the microscopic solver is used at specific grid points (red) to assist the macroscopic solution. Several PWC-based coupling methods (for both solids and fluids) have been proposed based on the above description. These differ in the involvement of the molecular solver and the means by which the properties in question are computed and can be generalised into two categories.

1. Heterogeneous multiscale method
2. Equation-free approach

(a) Patch dynamics
(b) Gap-tooth method

These are described in the following sections.

4.2.1 Heterogeneous multiscale method

The heterogeneous multiscale method (HMM) (Enguist and others 2003) assumes knowledge of the physical, continuum equations required for the calculation and evolution of the flow field. As the macroscopic field is not explicitly known across the entire domain, there is often a lack of data essential for the solution of these equations, e.g. stress tensor. The microscopic solver provides the relevant information.

For modelling the physical system, the following should be considered

- The continuum model to be used.
- The data computed by the microscopic solver to be fed into the macroscopic model.
- Conversion of a continuum state into a consistent microstate (as explained in Sect. 4.1.1).
- Conversion of averaging a microstate to realise the continuum value.

The system is then advanced based on the following steps:

From a macroscopic state variable U, the microstate is reconstructed by adjusting the positions and momenta of the atoms.

1. Using the molecular solver, the system is evolved and the necessary data (usually stress tensor or slip condition) are computed.
2. The data are then inserted into the macroscopic model to realise the field at a later time

Initial implementations of HMM have successfully simulated phenomena such as homogenisation, dislocation dynamics, and crack propagation (Weinan et al. 2003). Subsequent studies have used such methods to model complicated flows, e.g. driven cavity flows (Ren and Weinan 2005). MD was used to calculate the stress tensor from first principles, using the Irving-Kirkwood formula, instead of relying on assumptions that are inaccurate for, Newtonian fluids. Hence, the investigation concludes that such approaches are suitable for complex fluids, e.g. polymeric fluids. Traditional formulation of HMM is unable to study steady state problems since the velocity field U, used to impose boundary conditions on the molecular solver, vanishes along with the time derivative in Eq. 2.4. Recent studies have circumvented this problem by using the Laplacian of the streaming velocity and temperature (Alexiadis et al. 2013) to calculate momentum and heat transfer. In addition, their method avoids using the complicated Irving-Kirkwood equations to calculate the stress tensor and, instead, uses the simpler "framed" cell approach

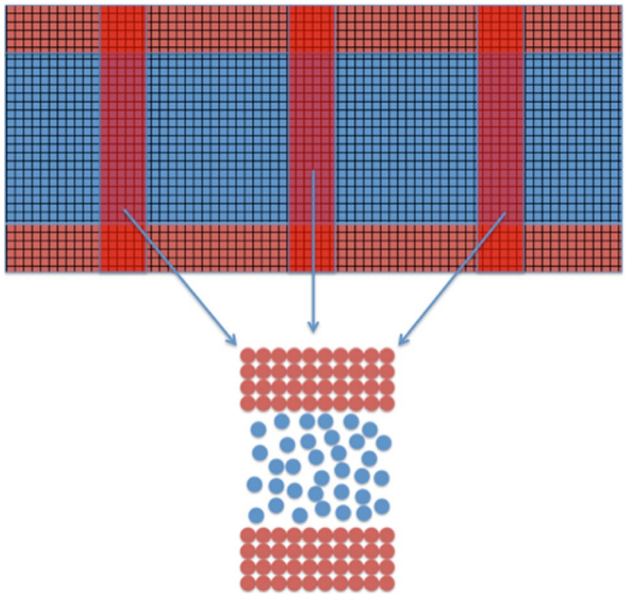

Fig. 11 Schematic representation of IMM. The entire channel is solved with a continuum solver. The molecular component is used over sparsely placed, thin regions, spanning the entire width of the channel

(Hadjiconstantinou and Patera 1997; Drikakis and Asproulis 2010). The approach was validated by simulating a flow through a channel under the effect of gravity.

A variation of the HMM is the internal-flow multiscale method (IMM), tailored for micro- and nanoflows through channels of high aspect ratios (Borg et al. 2012). The system is again treated entirely by the continuous solver. However, the microscopic component treats thin strips across the entire width of the channel rather than small regions around grid points (Fig. 11). The rationale is that for very narrow channels, the molecular regions of traditional HMM which need to have a minimum volume (depending on the mean free path of the system) might overlap introducing a computational overhead surpassing the computational expense of full MD. Rather than imposing the velocity field onto the molecular region, IMM imposes pressure gradient, emulated through an applied force.

The spacing between the molecular slices depends on the rate of change of the flow and geometric properties. The faster the change is, the closer these regions should be. Hence, such methods are not so effective in simulating channels interconnected through junctions where the geometry varies significantly within small length scales, a scenario which is quite common in engineering (e.g. reservoir inlet/exit junction). To accommodate such models, an extension of the model has been proposed which treats channels of high aspect ratio with IMM, while covering the junction components entirely through MD (Borg et al. 2013b). The IMM approach has further been adopted for compressible flows (Patronis et al. 2013) using the direct simulation Monte Carlo (DSMC) method.

Recent studies have introduced the fieldwise coupling (FWC) approach (Borg et al. 2013a), circumventing the limitation of traditional HMM methods in relatively coarse grids. In contrast to PWC that couples the molecular region to a node of the continuum grid, FWC couples the MD and CFD regions. MD simulations are used to calculate stress and velocity profiles within molecular domain and feed their values into the CFD solver. The microscopic elements can have an arbitrary position and size, hence increasing the versatility of the method for different characteristic system dimensions and enabling flow phenomena of varying length scales to be modelled. The HMM-FWC approach in conjunction with DSMC was also extended to model heat transfer problems in rarefied gases (Docherty et al. 2014).

To further improve the computational efficiency of PWC models, MD calculations can be cached into suitable data structures for use at a later time step (Asproulis and Drikakis 2013). If the information requested by the continuum model resembles previously processed data, then the molecular result is extracted from the cache, rather than requiring recomputing. Furthermore, artificial neural networks can be trained to optimise the volume of stored information and to minimise the molecular fluctuations.

4.2.2 *Equation-free approach*

The equation-free approach (EFA) is a PWC method, which circumvents the need for continuum closed-form equations (Kevrekidis et al. 2003, 2004). The main idea is that small bursts of appropriately initialised microscopic simulations can be used to calculate the same information that explicit continuum formulas would produce. The gap-tooth method defines small regions (referred to as "teeth") in space where the microscopic solver calculates desired observation variables (e.g. density) (Gear et al. 2003). Spatial interpolation between the calculations of these regions can compute the macroscopic field. This successfully decouples the microscopic and macroscopic spatial scales, but does nothing to decouple the time between them.

Patch dynamics can then be used to decouple timescales. In general, given the initial value of a property c, marked as c_0, as well as its time derivative $\frac{\mathrm{d}c}{\mathrm{d}t}$, one can use the forward Euler method

$$c_{n+1} = c_n + \tau \frac{\mathrm{d}c}{\mathrm{d}t} \tag{4.4}$$

to calculate the value of c at future times. Here, τ is the macroscopic time step. Although a model would normally be used for the derivative, the patch dynamics approach

calculates it by allowing the microscopic solver to run for a small period of time. We can then project the solution to the next macroscopic time step τ using the forward Euler method (or more generally a Taylor series). During this macroscopic time step, the molecular solver is not used at all. However, following the projection step, the microscopic simulation must be reinitialised accordingly to obtain the derivative for the next iteration. Since the molecular component runs for a short period of time, following the macroscopic time step, the patch dynamics approach also decouples the macro- and micro-timescales.

The macroscopic and microscopic time step used for the EFA can vary significantly depending on the problem to be modelled and the computational method employed. In fact, this approach is by no means restricted to a specific type of microscopic model. Many applications have used mesoscale models to compute the field in between projections for a wide range of applications. Using the LBM, previous studies investigated the interaction between arrays of bubbles in a two-phase liquid (Sankaranarayanan et al. 2002, 2003; Theodoropoulos et al. 2004). The EFA, in conjunction with the LBM, has also been used to study reaction–diffusion problems (Kevrekidis et al. 2003). Investigations have also used patch dynamics with kinetic Monte Carlo to study a model of heterogeneous catalytic surface reactions (Makeev et al. 2002; Siettos et al. 2003).

Although the above investigations have demonstrated that this method is effective, it is usually restricted to problems where the macroscopic physics are not well understood. In the case where continuum, closed-form equations are available, HMCM such as GD or HMM are preferred.

5 Conclusions

The recent academic and industrial interest in micro- and nanofluidic devices has necessitated the development of computational strategies that can assist the design of such devices. From the perspective of the physical understanding of such systems, the high-resolution molecular methods are ideal approaches. Their computational cost, however, significantly limits their use to systems containing a modest number of atoms. For larger scales, the computational efficiency of continuum methods such as CFD is particularly appealing, but the steep gradients and discontinuities characterising microflows are beyond the scope of the Navier–Stokes equations.

This review presented the efforts for the design of computational models attempting to bridge the gap between accuracy and computational efficiency. Various mesoscale models, which provide an intermediate resolution for computation, and hybrid methods, which use both molecular and continuum solvers for the description of the fluid field, were presented. To date, there is no universal method, which covers all regimes. The appealing simplicity of the LGA is compromised by the discrete nature of the velocities and density, which produces unrealistic physical phenomena for complex systems. Although the more refined LBM has been improved significantly over the years to include various effects, e.g. multiphase flows, boundary conditions, disadvantages emerging from the limitation of lattice-based system dynamics still exist. As a coarse-grained version of MD, DPD is an appealing method with the capability of providing an accurate representation of complex systems. However, depending on the grouping of the molecules, the dissipative pseudo-particles, interatomic and intermolecular interactions can be blurred.

HMCM provide a good comprise by using both solvers. Complications arise, however, in the choice of the regions in which the molecular solver will be applied. GD, for example, might not be appropriate in systems where the entire channel is governed by microscopic phenomena, and therefore, the definition of a continuum region is not possible without compromising accuracy. PWC-based approaches generally seem to be the most versatile, potentially providing information across the entire domain. However, when the geometries and gradients vary significantly within small length scales, the number of molecular regions needs to increase, which can quickly add to the overall computational expense.

For highly variable geometries and gradients, the number of molecular regions needs to increase, which can quickly add to the computational expense. Furthermore, no mesoscale or HMCM methods are capable of dealing efficiently and effectively with problems in which the molecular timescales are comparable to and greater than the macroscopic ones. Phenomena falling within this category are adsorption and sedimentation. Whether such physical behaviour can be simulated using multiscale approaches is yet to be seen.

Finally, although significant advances in multiscale modelling are yet to be made, the efforts of the last three decades have facilitated a number of options, which can be considered for a large spectrum of flow regimes of interest in engineering.

Compliance with ethical standards

Conflict of interest We confirm that there are no potential conflicts of interest or research involving human participants and/or animals.

References

Alexiadis A, Lockerby DA, Borg MK, Reese JM (2013) A Laplacian-based algorithm for non-isothermal atomistic-continuum hybrid

simulation of micro and nano-flows. Comput Methods Appl Mech Eng 264:81–94
Allen MP, Tildesley DJ (1989) Computer simulation of liquids. Oxford University Press, Oxford
Asproulis N, Drikakis D (2010) Boundary slip dependency on surface stiffness. Phys Rev E 81:061503
Asproulis N, Drikakis D (2011) Wall-mass effects on hydrodynamic boundary slip. Phys Rev E 84:031504
Asproulis N, Drikakis D (2013) An artificial neural network-based multiscale method for hybrid atomistic-continuum simulations. Microfluid Nanofluid 15:559–574
Asproulis N, Kalweit M, Shapiro E, Drikakis D (2009) Mesoscale flow and heat transfer modelling and its application to liquid and gas flows. J Nanophotonics 3(1):031960
Asproulis N, Kalweit M, Drikakis D (2012) A hybrid molecular continuum method using point wise coupling. Adv Eng Softw 46(1):85–92
Baranyai A, Evans DJ, Daivis PJ (1992) Isothermal shear-induced heat flow. Phys Rev A 46:7593
Barrat J-L, Chiaruttini F (2003) Kapitza resistance at the liquid–solid interface. Mol Phys 101:1605–1610
Barsky S, Delgado-Buscalioni R, Coveney PV (2004) Comparison of molecular dynamics with hybrid continuum–molecular dynamics for a single tethered polymer in a solvent. J Chem Phys 121:2403–2411
Barton P, Kalweit M, Drikakis D, Ball G (2011) Multi-scale analysis of high-speed dynamic friction. J Appl Phys 110(9):093520
Bhatnagar PL, Gross EP, Krook M (1954) A model for collision processes in gases. I. Small amplitude processes in charged and neutral one-component systems. Phys Rev 94(3):511
Bitsanis I, Magda J, Tirrell M, Davis H (1987) Molecular dynamics of flow in micros. J Chem Phys 87:1733–1750
Borg MK, Lockerby DA, Reese JM (2012) A multiscale method for micro/nano flows of high aspect ratio. J Comput Phys 233:400–413
Borg MK, Lockerby DA, Reese JM (2013a) Fluid simulations with atomistic resolution: a hybrid multiscale method with field-wise coupling. J Comput Phys 255:149–165
Borg MK, Lockerby DA, Reese JM (2013b) A hybrid molecular-continuum simulation method for incompressible flows in micro/nanofluidic networks. Microfluid Nanofluid 15:541–557
Chen S, Doolen GD (1998) Lattice Boltzmann method for fluid flows. Annu Rev Fluid Mech 30(1):329–364
Choi C-H, Westin KJA, Breuer KS (2003) Apparent slip flows in hydrophilic and hydrophobic microchannels. Phys Fluids 15:2897–2902
De Fabritiis G, Delgado-Buscalioni R, Coveney PV (2004) Energy controlled insertion of polar molecules in dense fluids. J Chem Phys 121:12139–12142
De Fabritiis G, Serrano M, Delgado-Buscalioni R, Coveney PV (2007) Fluctuating hydrodynamic modeling of fluids at the nanoscale. Phys Rev E 75:026307
Delgado-Buscalioni R, Coveney P (2003a) Continuum-particle hybrid coupling for mass, momentum, and energy transfers in unsteady fluid flow. Phys Rev E 67:046704
Delgado-Buscalioni R, Coveney P (2003b) USHER: an algorithm for particle insertion in dense fluids. J Chem Phys 119:978–987
Delgado-Buscalioni R, Coveney PV (2004) Hybrid molecular-continuum fluid dynamics. Philos Trans R Soc London A Math Phys Eng Sci 362:1639–1654
Delgado-Buscalioni R, Flekkøy EG, Coveney PV (2005) Fluctuations and continuity in particle-continuum hybrid simulations of unsteady flows based on flux-exchange. Europhys Lett 69:959
Docherty SY, Borg MK, Lockerby DA, Reese JM (2014) Multiscale simulation of heat transfer in a rarefied gas. Int J Heat Fluid Flow 50:114–125
Doerr A, Tolan M, Seydel T, Press W (1998) The interface structure of thin liquid hexane films. Phys B 248:263–268
Drikakis D, Asproulis N (2010) Multi-scale computational modelling of flow and heat transfer. Int J Numer Meth Heat Fluid Flow 20(5):517–528
Enguist B et al (2003) The heterogeneous multi-scale methods. Commun Math Sci 1:87–133
Filippova O, Hänel D (1998) Grid refinement for lattice-BGK models. J Comput Phys 147(1):219–228
Flekkøy EG, Wagner G, Feder J (2000) Hybrid model for combined particle and continuum dynamics. Europhys Lett 52:271
Gear CW, Li J, Kevrekidis IG (2003) The gap-tooth method in particle simulations. Phys Lett A 316(3):190–195
Guo Z, Zheng C, Shi B (2002a) An extrapolation method for boundary conditions in lattice Boltzmann method. Phys Fluids 14(6):2007–2010
Guo Z, Zheng C, Shi B (2002b) Discrete lattice effects on the forcing term in the lattice Boltzmann method. Phys Rev E 65(4):046308
Hadjiconstantinou NG (1999) Hybrid atomistic–continuum formulations and the moving contact-line problem. J Comput Phys 154:245–265
Hadjiconstantinou NG, Patera AT (1997) Heterogeneous atomistic-continuum representations for dense fluid systems. Int J Mod Phys C 8:967–976
Hardy J, Pomeau Y, De Pazzis O (1973) Time evolution of a two-dimensional model system. I. Invariant states and time correlation functions. J Math Phys 14(12):1746–1759
Henderson J, van Swol F (1984) On the interface between a fluid and a planar wall: theory and simulations of a hard sphere fluid at a hard wall. Mol Phys 51:991–1010
Hoogerbrugge P, Koelman J (1992) Simulating microscopic hydrodynamic phenomena with dissipative particle dynamics. EPL Europhys Lett 19(3):155
Hyvaluoma J, Harting J (2008) Slip flow over structured surfaces with entrapped microbubbles. Phys Rev Lett 100(24):246001
Izquierdo S, Martinez-Lera P, Fueyo N (2009) Analysis of open boundary effects in unsteady lattice Boltzmann simulations. Comput Math Appl 58(5):914–921
Jones J, áNoel Ruddock J, Spenley N et al (1999) Dynamics of a drop at a liquid/solid interface in simple shear fields: a mesoscopic simulation study. Faraday Discuss 112:129–142
Kalweit M, Drikakis D (2008a) Coupling strategies for hybrid molecular–continuum simulation methods. Proc Inst Mech Eng C J Mech Eng Sci 222:797–806
Kalweit M, Drikakis D (2008b) Multiscale methods for micro/nano flows and materials. J Comput Theor Nanosci 5:1923–1938
Kalweit M, Drikakis D (2010) On the behaviour of fluidic material at molecular dynamics boundary conditions used in hybrid molecular–continuum simulations. Mol Simul 36(9):657–662
Kalweit M, Drikakis D (2011) Multiscale simulation strategies and mesoscale modelling of gas and liquid flows. IMA J Appl Math 76(5):661–671
Kevrekidis IG et al (2003) Equation-free, coarse-grained multiscale computation: enabling mocroscopic simulators to perform system-level analysis. Commun Math Sci 1(4):715–762
Kevrekidis IG, Gear CW, Hummer G (2004) Equation-free: the computer-aided analysis of complex multiscale systems. AIChE J 50(7):1346–1355
Kim BH, Beskok A, Cagin T (2008) Thermal interactions in nanoscale fluid flow: molecular dynamics simulations with solid–liquid interfaces. Microfluid Nanofluid 5:551–559
Ko S-H et al (2014) Numerical methodologies for investigation of moderate-velocity flow using a hybrid computational fluid dynamics–molecular dynamics simulation approach. J Mech Sci Technol 28:245–253

Kong Y, Manke C, Madden W, Schlijper A (1994) Simulation of a confined polymer in solution using the dissipative particle dynamics method. Int J Thermophys 15(6):1093–1101

Koplik J, Banavar JR, Willemsen JF (1989) Molecular dynamics of fluid flow at solid surfaces. Phys Fluids A Fluid Dyn 1:781–794 **(1989–1993)**

Koumoutsakos P (2005) Multiscale flow simulations using particles. Annu Rev Fluid Mech 37:457–487

Ladd AJ (1994) Numerical simulations of particulate suspensions via a discretized Boltzmann equation. Part 1. Theoretical foundation. J Fluid Mech 271:285–309

Liu Y, Wang Q, Zhang L, Wu T (2005) Dynamics and density profile of water in nanotubes as one-dimensional fluid. Langmuir 21:12025–12030

Liu M, Meakin P, Huang H (2006) Dissipative particle dynamics with attractive and repulsive particle–particle interactions. Phys Fluids 18(1):017101

Liu M, Meakin P, Huang H (2007) Dissipative particle dynamics simulation of multiphase fluid flow in microchannels and microchannel networks. Phys Fluids 19(3):033302

Liu J, Chen S, Nie X, Robbins MO (2008) A continuum-atomistic multi-timescale algorithm for micro/nano flows. Commun Comput Phys 4:1279–1291

Lyshevski SE (2005) Nano-and micro-electromechanical systems: fundamentals of nano-and microengineering, 8th edn. CRC Press, Boca Raton

Makeev AG, Maroudas D, Panagiotopoulos AZ, Kevrekidis IG (2002) Coarse bifurcation analysis of kinetic Monte Carlo simulations: a lattice-gas model with lateral interactions. J Chem Phys 117(18):8229–8240

McNamara GR, Zanetti G (1988) Use of the Boltzmann equation to simulate lattice-gas automata. Phys Rev Lett 61(20):2332–2335

O'Connell ST, Thompson PA (1995) Molecular dynamics–continuum hybrid computations: a tool for studying complex fluid flows. Phys Rev E 52:R5792

Patronis A, Lockerby DA, Borg MK, Reese JM (2013) Hybrid continuum-molecular modelling of multiscale internal gas flows. J Comput Phys 255:558–571

Pomeau BHY, Frisch U (1986) Lattice-gas automata for the Navier–Stokes equation. Phys Rev Lett 56(14):1505

Qian YH, d'Humières D, Lallemand P (1992) Lattice BGK models for Navier–Stokes equation. Europhys Lett 17(6):479

Ren W, Weinan E (2005) Heterogeneous multiscale method for the modeling of complex fluids and micro-fluidics. J Comput Phys 204:1–26

Revenga M, Zuniga I, Espanol P, Pagonabarraga I (1998) Boundary models in DPD. Int J Mod Phys C 9(8):1319–1328

Sankaranarayanan K, Shan X, Kevrekidis I, Sundaresan S (2002) Analysis of drag and virtual mass forces in bubbly suspensions using an implicit formulation of the lattice Boltzmann method. J Fluid Mech 452:61–96

Sankaranarayanan K et al (2003) A comparative study of lattice Boltzmann and front-tracking finite-difference methods for bubble simulations. Int J Multiph Flow 29(1):109–116

Sbragaglia M, Chen H, Shan X, Succi S (2009) Continuum free-energy formulation for a class of lattice Boltzmann multiphase models. Europhys Lett 86(2):24005

Shan X, Chen H (1994) Simulation of nonideal gases and liquid-gas phase transitions by the lattice Boltzmann equation. Phys Rev E 49(4):2941

Siettos C, Armaou A, Makeev A, Kevrekidis I (2003) Microscopic/stochastic timesteppers and "coarse" control: a kMC example. AIChE J 49(7):1922–1926

Sofos F, Karakasidis T, Liakopoulos A (2009) Transport properties of liquid argon in krypton nanochannels: anisotropy and non-homogeneity introduced by the solid walls. Int J Heat Mass Transf 52:735–743

Succi S (2001) The Lattice-Boltzmann equation. Oxford University Press, Oxford

Swift MR, Osborn W, Yeomans J (1995) Lattice Boltzmann simulation of nonideal fluids. Phys Rev Lett 75(5):830

Theodoropoulos C, Sankaranarayanan K, Sundaresan S, Kevrekidis I (2004) Coarse bifurcation studies of bubble flow Lattice Boltzmann simulations. Chem Eng Sci 59(12):2357–2362

Todd B, Evans DJ (1997) Temperature profile for Poiseuille flow. Phys Rev E 55:2800

Travis KP, Todd B, Evans DJ (1997) Departure from Navier–Stokes hydrodynamics in confined liquids. Phys Rev E 55:4288

Tuckerman DB, Pease R (1981) High-performance heat sinking for VLSI. Electron Device Lett IEEE 2:126–129

Wagner G, Flekkøy E, Feder J, Jøssang T (2002) Coupling molecular dynamics and continuum dynamics. Comput Phys Commun 147:670–673

Wang M, Liu J, Chen S (2008) Electric potential distribution in nanoscale electroosmosis: from molecules to continuum. Mol Simul 34:509–514

Weinan E, Engquist B, Huang Z (2003) Heterogeneous multiscale method: a general methodology for multiscale modeling. Phys Rev B 67:092101

Werder T, Walther JH, Koumoutsakos P (2005) Hybrid atomistic–continuum method for the simulation of dense fluid flows. J Comput Phys 205:373–390

Wijesinghe HS, Hadjiconstantinou NG (2004) Discussion of hybrid atomistic-continuum methods for multiscale hydrodynamics. Int J Multiscale Comput Eng 3:189–202

Willemsen S, Hoefsloot H, Iedema P (2000) No-slip boundary condition in dissipative particle dynamics. Int J Mod Phys C 11(5):881–890

Wolfram S (1986) Cellular automaton fluids 1: basic theory. J Stat Phys 45:471–526

Yu D, Mei R, Shyy W (2005) Improved treatment of the open boundary in the method of Lattice Boltzmann equation: general description of the method. Prog Comput Fluid Dyn Int J 5(1):3–12

Yunus NAM, Green NG (2010) Fabrication of microfluidic device channel using a photopolymer for colloidal particle separation. Microsyst Technol 16:2099–2107

Zou Q, He X (1997) On pressure and velocity boundary conditions for the lattice Boltzmann BGK model. Phys Fluids 9(6):1591–1598